Bone Reports 15 (2021) 101123

Contents lists available at ScienceDirect

Bone Reports

journal homepage: www.elsevier.com/locate/bonr

Gut microbiome depletion and repetitive mild traumatic brain injury differentially modify bone development in male and female adolescent rats

Ker Rui Wong [a,1], Marissa Sgro [a,1], Glenn R. Yamakawa [a], Crystal Li [a], Stuart J. McDonald [a,c], Mujun Sun [a], Sandy R. Shultz [a,b], Rhys D. Brady [a,b], Richelle Mychasiuk [a,*]

[a] Department of Neuroscience, Central Clinical School, Monash University, Melbourne, VIC, Australia
[b] Department of Medicine, Royal Melbourne Hospital, The University of Melbourne, Parkville, VIC, Australia
[c] Department of Physiology, Anatomy and Microbiology, School of Life Sciences, La Trobe University, Bundoora, VIC, Australia

ARTICLE INFO

Keywords:
Antibiotics
Concussion
Femur
Musculoskeletal
Sex differences

ABSTRACT

Dysregulation of the gut microbiome has been shown to disrupt both bone formation and bone resorption in several preclinical and clinical models. However, the role of microbiome in adolescent bone development remains poorly understood. This effect of disrupted bone development may be more pronounced during adolescence, when bone development is vulnerable to environmental stimuli and external insults (e.g., antibiotic treatment and traumatic brain injury), as this is a critical window of development. Therefore, in this study, we sought to investigate the effect of repetitive mild traumatic brain injury (RmTBI) and gut microbiome depletion by antibiotic treatment on femur length and bone density in male and female adolescent Sprague Dawley rats. Rats were randomly assigned to receive standard or antibiotic autoclaved drinking water and to receive sham or RmTBIs injuries. Using micro-computed tomography (μCT), we found sexually dimorphic changes in adolescent bone development in response to microbiome depletion and RmTBI. Specifically, gut microbiome depletion stunted femur growth in males and altered cross sectional bone area (CSA), bone area fraction, and the bone volume of low and mid density bone in the distal metaphyseal region of the femur. Conversely, RmTBI and antibiotic treatment individually disrupted bone growth, bone area fraction, and bone volume of high-density bone within the distal metaphyseal region of the femur in females, but not when combined. Therefore, findings from this study indicate that gut microbiome and RmTBI may alter bone development in a sex-dependent manner during adolescence.

1. Introduction

The microorganisms that colonise the small and large intestine, known as the gut microbiome, play an integral role in the development, function, and communication between the gut, brain, and immune system (the gut-brain-immune axis) (Cowan et al., 2020). Adolescence encompasses an important critical window of gut microbiome development; displaying high vulnerability to environmental stimuli (Paus et al., 2008). Environmental insults, including antibiotic administration, can result in dysbiosis, altering the composition and diversity of the gut microbiome (Ibáñez et al., 2019; Borre et al., 2014), which in turn impairs functioning of this delicately balanced system. Under normal conditions, gut bacteria are beneficial and play an important role in maintaining intestinal homeostasis and appropriate immune system function by regulating the inflammatory response (Ding et al., 2020).

Evidence also suggests that the gut microbiome influences bone growth, bone mass acquisition, and maintenance; similarly known as the microbiome-bone relationship or gut-microbiota-bone axis (Xu et al., 2017; Medina-Gomez, 2018). Although the exact mechanisms by which the gut microbiome regulates bone health remain speculative, it is believed that the microbiome plays a significant role in nutrient absorption, thereby influencing bone growth, bone mass acquisition, and remodeling (Xu et al., 2017; Hernandez et al., 2016; Yan and Charles, 2017; Li et al., 2016). Given that bone mass acquisition increases during adolescence, alterations during this sensitive period, may lead to significant long-term complications, such as disorders associated with low

* Corresponding author at: Department of Neuroscience, Central Clinical School, Monash University, 6th Floor, 99 Commercial Road, Melbourne, VIC 3004, Australia.
E-mail address: Richelle.mychasiuk@monash.edu (R. Mychasiuk).
[1] Authors contributed equally.

https://doi.org/10.1016/j.bonr.2021.101123
Received 12 July 2021; Received in revised form 14 August 2021; Accepted 27 August 2021
Available online 8 September 2021

bone mineral density including osteopenia and osteoporosis later in life (Ibáñez et al., 2019; Gokhale et al., 1998). Importantly, bone mineral density continues to increase until peak bone mass is acquired in adolescence (Rauch and Schoenau, 2001).

In addition, insults such as a mild traumatic brain injury (mTBI) and repetitive mTBI (RmTBI), have also been shown to alter the gut-brain-immune axis. For example, research has demonstrated that mTBI-induced dysregulation of the gut-brain-immune axis and hypothalamic pituitary adrenal (HPA) axis, initiate an inflammatory response systemically and within the gut (Jin et al., 2008). Inflammation within the gut further exacerbates dysbiosis, amplifying deficits in gut bacteria that function to regulate HPA axis function (Sudo et al., 2004), vagal nerve stimulation (Bonaz et al., 2018), short chain fatty acid (SCFA) secretion, microglia activation (Erny et al., 2015), and blood brain barrier (BBB) permeability (Strandwitz, 2018). If insults such as RmTBI during adolescence disrupt the gut-brain-immune axis, they may also interfere with bone resorption and formation, resulting in alterations to bone volume and the development of bone.

Although not generally examined, but of particular importance, sexual dimorphism exists in bone development (Xu et al., 2017; Olson et al., 2011; Warden et al., 2005), maturation of the gut-brain-immune axis (Yurkovetskiy et al., 2013; Chen and Madak-Erdogan, 2016), and the presentation of symptomologies following RmTBI (Rosenbaum and Lipton, 2012). Therefore, the purpose of this study was to investigate the effects of microbiome depletion and RmTBI on bone development in male and female adolescent rats. Given that we previously identified bone loss 7 days following a moderate TBI (Brady et al., 2016a), we examined femur length, overall bone mineral density, bone volume ratio at three different densities as well as morphological and biomechanical parameters within the distal metaphyseal region of the femur in adolescent Sprague Dawley rats exposed to microbiome depletion (via antibiotic administration), RmTBI, or combination of both. Given the role of the microbiome and RmTBI in neuroinflammation and nutrient absorption, we hypothesized that rats with depleted microbiomes would exhibit reduced femur length and bone volume, while rats that experienced both RmTBI and microbiome depletion would exhibit further restriction of femur growth and impairments in bone volume.

2. Methods

2.1. Animals and gut microbiome depletion treatment

Thirty-five adolescent males and 28 adolescent females postnatal (P) day 21 Sprague Dawley rats (total $n = 63$) were obtained from the Monash Animal Research Platform (Clayton, Victoria, Australia). All animal procedures were approved by the Alfred Medical Research and Educational Precinct (AMREP) Animal Ethics Committee (E/1992/2020/M). At P21, adolescent male and female Sprague Dawley rats were randomly assigned to either antibiotic or standard autoclaved drinking water. The antibiotic cocktail administered in their drinking water consisted of ampicillin (1 g/L), vancomycin (500 mg/L), imipenem (250 mg/L), metronidazole (1 g/L), and ciprofloxacin HCL (20 mg/L). This antibiotic cocktail was previously described in Hoban et al. (2016) to effectively deplete the gut microbiota following a 14 day administration protocol. The antibiotic cocktail was administered for 14 days (P21-P35). Rats on antibiotic water were transferred back to standard autoclaved drinking water on P36 for the remainder of the study.

2.2. RmTBI induction – lateral impact device

Rats in each group were randomised to receive 3 mTBIs or sham injuries at P37, P39, and P41. Males (Placebo + Sham; $n = 7$), (Placebo + RmTBI; $n = 6$), (Antibiotics + Sham; $n = 11$), (Antibiotics + RmTBI; n = 11). Females (Placebo + Sham; $n = 7$), (Placebo + RmTBI; n = 7), (Antibiotics + Sham; n = 7), (Antibiotics + RmTBI; n = 7). Sham and RmTBI injuries were administered using the lateral impact (LI) device, as previously described (Mychasiuk et al., 2016). Specifically, rats were anaesthetized with 5% isoflurane and placed chest down on a low friction Teflon® board. With the left temporal lobe facing the impactor, a 50-g weight was propelled toward the rat's head using pneumatic pressure at an average speed of 8.39 ± 0.31 m/s, inducing mTBIs at ~85.52 Gs. The weight impacted a small aluminium 'helmet' to prevent damage to the skull whilst still propelling the rat into a horizontal 180° rotation across the Teflon® board. Following impact, the rat was removed from the device and placed on its back in a clean, warm cage to recover. This LI technique is a clinically relevant model that emulates the acceleration and rotational forces of sports-related concussion (Mychasiuk et al., 2016). The amount of time required for the rat to wake up and flip from a supine to a prone position (time-to-right) was recorded as a measure of loss of consciousness (Fig. 1B).

2.3. Femur collection (tissue processing)

Rats were euthanised at P52 for femur collection. Rats were transcardially perfused with 1× PBS and 4% PFA, the contralateral femur bones were removed, placed in 4% PFA, and stored at 5 °C for 3 days before being transferred into 70% ethanol and placed back into storage at 5 °C. Considering the overlap in development between the gut microbiome and skeletal bone, bone mineral density and femur length was analysed by micro-computed tomography (μCT).

2.4. Micro-computed tomography (μCT) scanning of femurs

Prior to scanning, femurs were rehydrated in 0.9% saline solution overnight and wrapped in cotton gauze moistened in saline, which prevented sample movement and dehydration during scanning.

Bones were scanned using a SkyScan 1276 scanner (Bruker MicroCT), using the following settings: 9-μm voxel resolution, 0.25 mm aluminium filter, 70 kV voltage, 180 μA current, 400-ms exposure time, rotation 0.5° across rotation, frames averaging of 3.

Images were then reconstructed using NRecon (version 1.7.4.6) with the following parameters: smoothing: 1, ring artefact reduction: 6, beam hardening compensation: 35%, CS rotation: automatic, attenuation coefficient (density): 0–0.07.

Following reconstruction, images were re-oriented using DataViewer (version 1.5.0), ensuring that a consistent region of interest (ROI) was selected throughout the study (Walker et al., 2020). The centre of the distal growth plate was first located using the coronal plate, followed by symmetrical arrangement of the four quadrants of the cross-sectional growth plate in the transaxial plate.

Transaxial datasets with corrected orientations were then used to determine ROI (Fig. 2A), volume of interest (VOI), multilevel thresholding and morphometric analysis using Skyscan CT-Analyzer (CTAn) (version 1.20.3.0, Bruker MicroCT software). Pseudocoloured images were used to visualise changes in bone densities across different treatment and injuries using CTvox (version 3.3.1) (Fig. 3A).

Length of the metaphyseal ROI for each sample was first determined by measuring the femur length, thus ensuring that the same anatomical region was selected regardless of the differences in bone length. The distal end of ROI was defined as 10% of the femur length, extending from the growth plate, a region which has been found to encompass secondary spongiosa and is typically used to investigate bone microarchitecture (Williams et al., 2020). The proximal end of the ROI was determined as a further 15% region extending from the distal end of ROI (Fig. 2A). An elliptical region, containing both trabecular and cortical bone within the ROI was then selected for the first and last slice, interpolated by the software.

To analyse overall bone features we employed morphometric 2-dimensional (2-D) analysis using adaptive pre-thresholding in CTan with thresholds set at 66 – 255, radius of 7, and constant of 0. These parameters include: mean bone mineral density (BMD), polar moment of inertia, cross-sectional bone area (CSA), cross-sectional tissue area

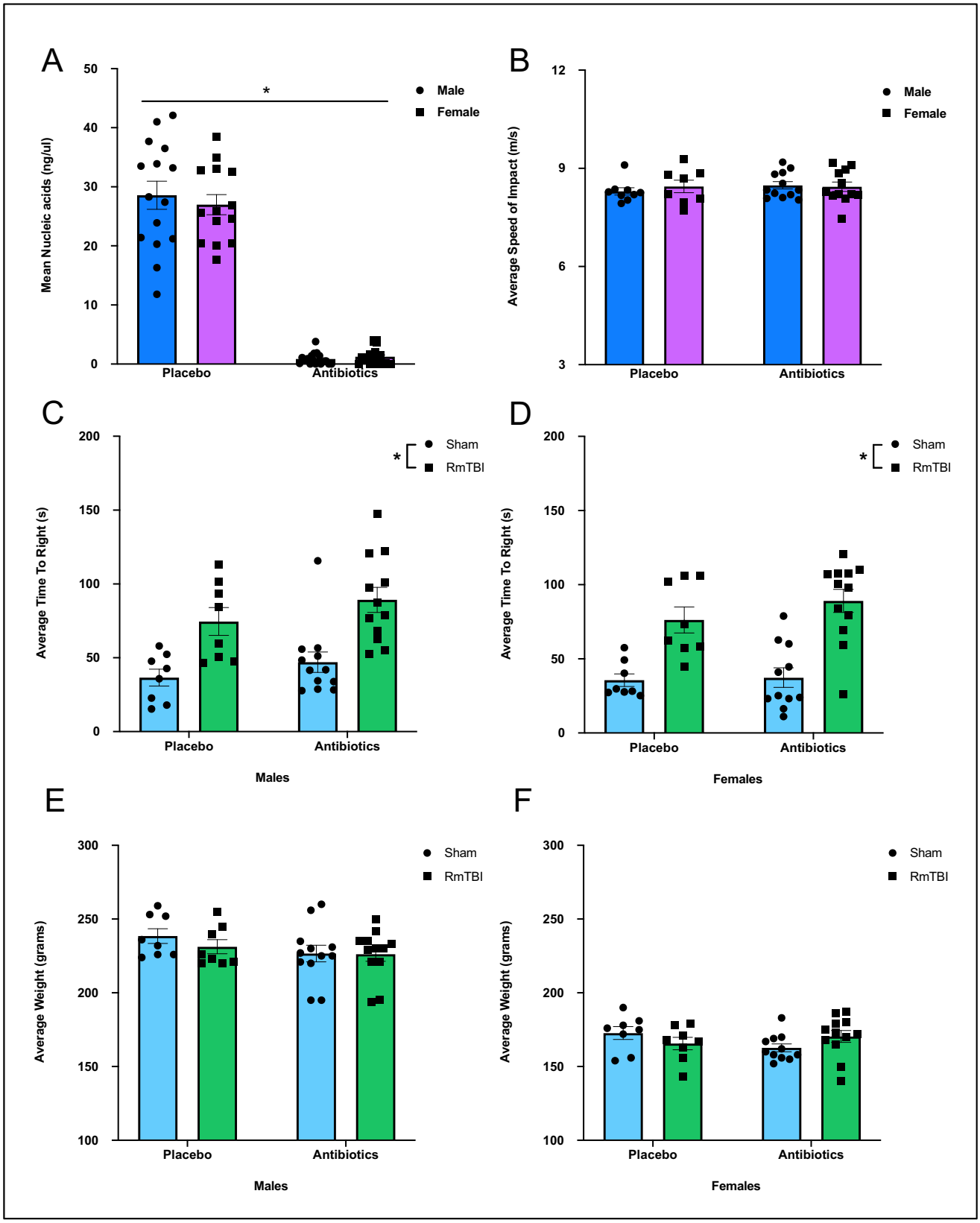

Fig. 1. Confirmation of depleted gut microbiome (A), average speed of impact for RmTBIs (B), confirmation of injury induction (C, D) and average weight at time of femur collection (E, F). Both male and female rats on the antibiotic cocktail had a significantly reduced mean nucleic acid concentration confirming gut microbiome depletion (A). All rats received RmTBI at similar impact speeds (B). Male and female rats that received RmTBI demonstrated significantly longer time-to-rights compared to sham injured rats (C, D). No significant effects were found in average weight in males (E) or females (F) at time of femur collection (euthanasia). Graphs are shown as mean of each group ± SEM, * represent significant difference, $p < .050$.

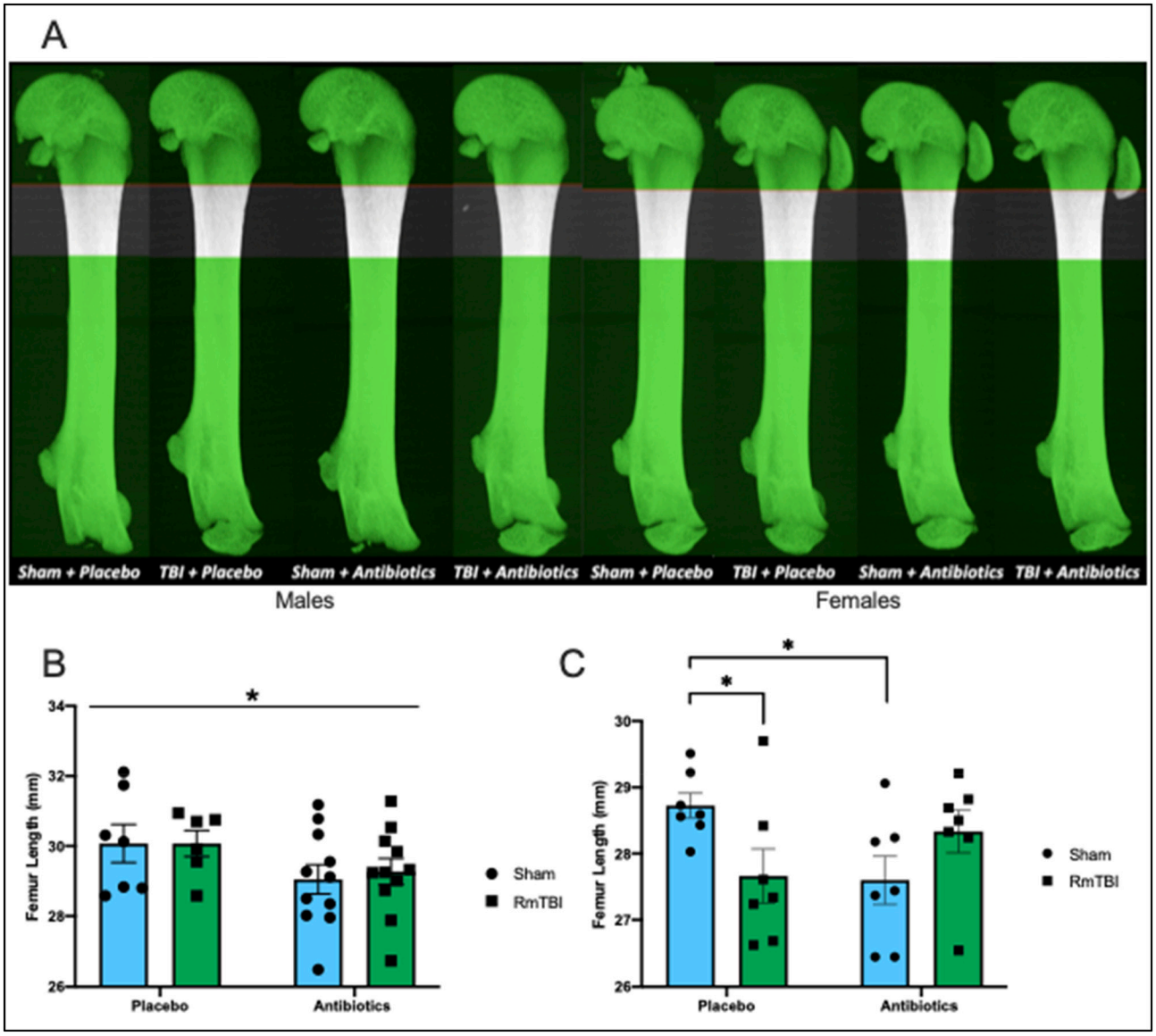

Fig. 2. Representative projection of male and female femurs from each treatment and injury groups, with region of interest (ROI) shown (A). Region of interest begins at 10% of the femur length away from the growth plate, extending an additional 15% of the femur length. There was significant treatment effect where femur length for male rats that were treated with antibiotics was reduced when compared to placebo treated male rats. No difference was observed between injury groups (B). Antibiotic treatment significantly reduced femur length of female sham rats when compared to placebo treated sham rats. Similarly, RmTBI also reduces femur length in the female placebo-treated group (C). Graphs are shown as mean of each group ± SEM, * represent significant difference, $p < .050$.

(CTA), and bone area fraction (B.Ar/T.Ar).

To gain a greater understanding of the morphological changes occurring, additional analyses was performed where bone was automatically segregated into low, mid, and high density via multilevel Otsu thresholding. Given the number of groups and interventions, analysis of bone at a single threshold would have obscured information about the mineral content of the bone material. In addition, single threshold analyses rely on normal morphology to separately analyse cortical and trabecular structures. Due to the nature of the interventions and our a-priori hypotheses that these would result in significant changes in bone morphology, the morphology could not be considered "normal". We therefore used multilevel Otsu thresholding to establish thresholds for measuring bone volume fraction at low, mid, and high density to control for significant heterogeneity between sexes, as well as treatment and injury groups (Walker et al., 2020; Walker et al., 2021). This iterative algorithm separates pixels from raw images based on mean grey level intensity into different classes (Otsu, 1979).

For this study, multilevel Otsu thresholding was applied across VOI of male controls (Sham + Placebo) and female controls (Sham + Placebo), to categorize the grey pixels into 4 threshold levels, representative of the densities for other treatment groups. The threshold levels were calibrated to calcium hydroxyapatite reference phantoms (Bruker Micro-CT, Kontich, Belgium): low density: 0.194–0.548 g/cm^3, mid density: 0.548–0.930 g/cm^3, high density: > 0.930 g/cm^3 for males, and low density: 0.201–0.576 g/cm^3, mid density: 0.576–0.970 g/cm^3, and high density: > 0.970 g/cm^3 for females. Measurements at the lowest density, < 0.194 g/cm^3 for males, and < 0.201 g/cm^3 for females, were treated as noise or background and were excluded. Male and female femurs were then analysed using the 3 density thresholds obtained from the male and female control groups. Bone volume over total tissue volume (BV/TV) at each density threshold was measured and expressed as a percentage.

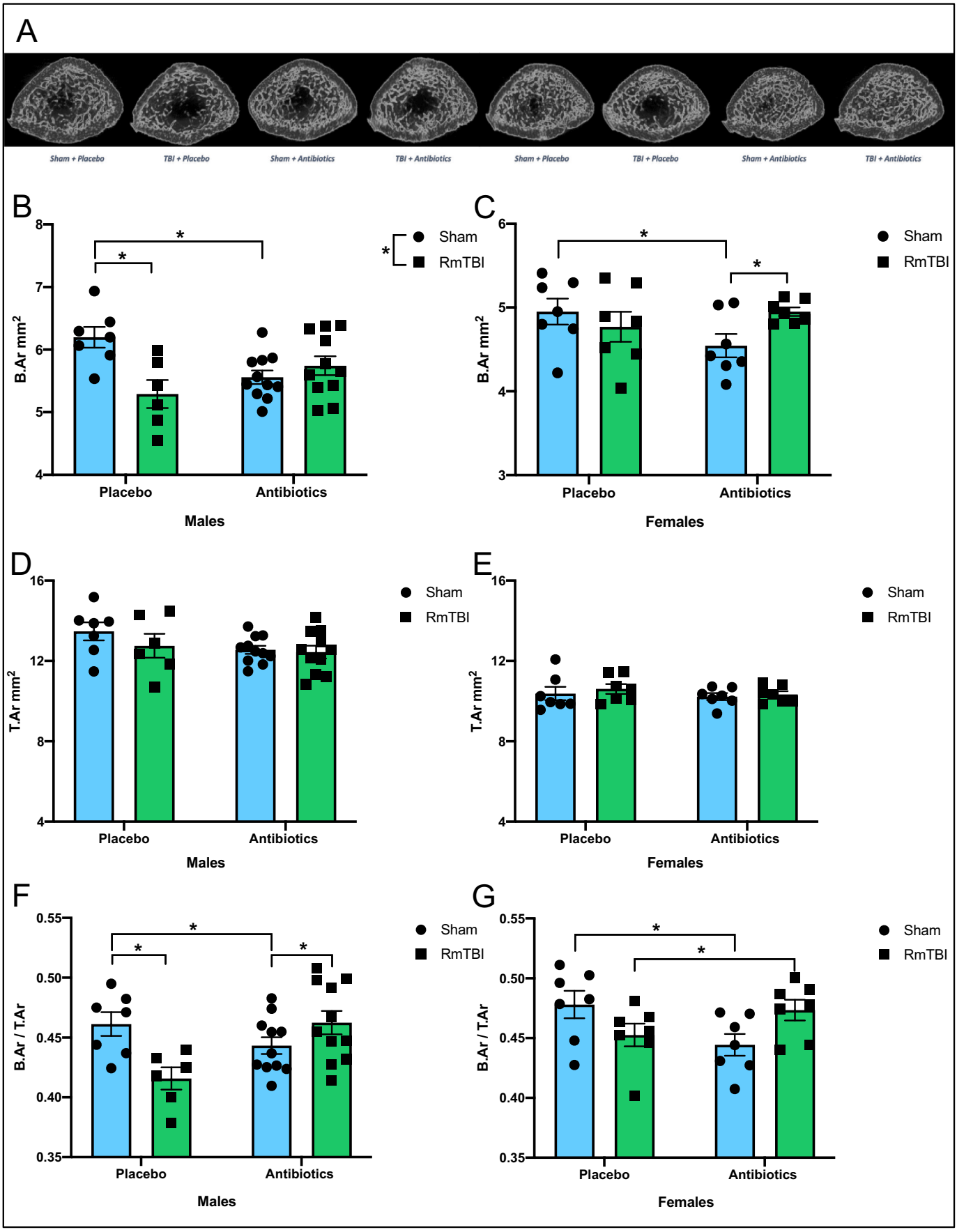

(caption on next page)

Fig. 3. Antibiotic administration and RmTBI differentially modify BSA and bone area fraction in male and female adolescent rats. Representative grayscale cross-sectional images (A). For male rats there was a significant injury and an injury by treatment interaction where antibiotic treatment and RmTBI alone, both resulted in a reduction in CSA (B). There were no changes in CTA (D). For bone area fraction there was a significant injury by treatment interaction, with reductions in both placebo-treated RmTBI and antibiotic-treated sham rats but increased in males that experienced both antibiotics + RmTBI (F). For females, sham rats that received antibiotic treatment displayed reduced CSA when compared to placebo-treated sham rats, but CSA is increased in rats that experienced both antibiotics and RmTBI (C). There were no effects in CTA (E). Antibiotic treatment significantly reduced bone area fraction in sham rats, however, in rats that experienced both antibiotics and RmTBI, bone area fraction is increased (G).

2.5. Gut microbial DNA extraction from stool samples

Gut microbial DNA concentrations were obtained by collecting stool samples from the commencement of antibiotic administration to the completion of the study. After collection, stool samples were transferred to storage at −80 °C. Samples were thawed and gut bacteria was extracted using QIAGEN QIAamp Fast DNA Stool Mini Kit as described by manufactures instructions (Qiagen, Hilden Germany). The concentration and quality of bacterial DNA was measured with the QIAGEN QIAxpert Spectrophotometer using an absorbance ratio of A260/280 (Qiagen, Hilden Germany).

2.6. Statistical analyses

Power calculations were completed with G*Power software (version 3.1). Based upon Cohen's (1988) criteria (Cohen, 1992) and a moderate effect size of 0.4, alpha of 0.05, a power of 0.8, with eight groups, the estimated sample size needed for the entire study was $N = 52$. Two-way ANOVAs with injury (RmTBI; sham), and treatment (antibiotics; placebo), as factors were run for all measures using SPSS 25 for MAC. Post-hoc pairwise comparisons were run when appropriate. For all bone measurements, male and female animals were analysed separately due to inherent sex differences in bone density. All figures are displayed as means ± standard error and statistical significance was considered $p < .05$. Bone analyses were conducted by investigators blinded to treatment allocations. All data will be made available upon request from the corresponding author.

3. Results

3.1. Validation of microbiome depletion and injury

PCR analyses of bacterial DNA was used to determine if antibiotic administration was effective at depleting the microbiome. The two-way ANOVA with sex and treatment as factors demonstrated a main effect of treatment, $F(1, 79) = 437.301$, $p < .001$, but not of sex, indicating that all animals who consumed the antibiotic cocktail exhibited significant and complete depletion of bacterial DNA from their faecal samples. See Fig. 1A.

The two-way ANOVA with sex and treatment as factors demonstrated that there were no significant differences in the average speed of impact for the RmTBIs, $p > .050$. See Fig. 1B. The time-to-right following injury induction was used as a measure of loss of consciousness and confirmation that the animal did in fact receive a mild TBI. The three-way ANOVA for average time-to-right failed to demonstrate a main effect of sex or treatment ($p > .050$), but did exhibit a main effect of injury, $F(1, 79) = 61.383$, $p < .001$, whereby animals in the RmTBI group took longer to right themselves, than sham animals. See Fig. 1C and D. Finally, average body weight at the time of euthanasia (i.e. femur collection) is illustrated in Fig. 1E and F. The three-way ANOVA demonstrated a main effect of sex, $F(1, 79) = 304.643$, $p < .001$, with males weighing more than females, but not of injury or treatment, $p > .050$.

3.2. Femur length

3.2.1. Males

Antibiotic administration/microbiome depletion, significantly reduced femur length in adolescent males. The two-way ANOVA demonstrated a main effect of treatment, $F(1, 34) = 4.680$, $p = .038$, but not of injury, $F(1, 34) = 0.034$, $p = .856$. See Fig. 2B.

3.2.2. Females

Antibiotic administration interacted with RmTBI in adolescent females to modify femur length, whereby femur growth was reduced in placebo + RmTBI animals ($p = .033$), but increased in females that experience both antibiotics + RmTBI ($p = .024$), see Fig. 2C. The two-way ANOVA failed to exhibit a main effect of injury or treatment, p's > 0.050, although there was a significant treatment by injury interaction, $F(1, 28) = 7.367$, $p = .012$.

3.3. Overall bone features

3.3.1. Males

Antibiotic administration altered cross-sectional bone area and bone area fraction but not cross-sectional tissue area, see Fig. 3. For CSA, there was a significant main effect of injury, $F(1, 34) = 5.114$, $p = .031$, and a significant injury by treatment interaction, $F(1, 34) = 11.612$, $p = .002$, whereby both antibiotic treatment and RmTBI alone, resulted in a reduction in bone area (Fig. 3B). There were no significant changes in CTA, p's > 0.050 (Fig. 3C). For bone area fraction, there were no significant main effects, but we did identify a significant injury by treatment interaction, $F(1, 34) = 11.607$, $p = .002$, with post-hoc analyses exhibiting reduced bone area fraction in both placebo-treated RmTBI ($p = .005$) and antibiotic-treated sham rats ($p = .005$), but increased bone area fraction in antibiotic males that experienced RmTBIs ($p = .002$) (Fig. 3D).

3.3.2. Females

The two-way ANOVA for CSA demonstrated a significant treatment by injury interaction, $F(1, 27) = 4.393$, $p = .047$, whereby sham rats that received antibiotic treatment displayed reduced cross-sectional bone area when compared to placebo-treated sham rats, while bone area was increased in antibiotic rats that experienced RmTBIs (Fig. 3E). There were no significant effects or interactions for CTA, p's > 0.050 (Fig. 3F). Finally, the two-way ANOVA for bone area fraction in females demonstrated that antibiotic treatment reduced area in sham rats ($p = .004$), however, in rats that experienced both antibiotics and RmTBI, bone area fraction is increased ($p = .042$), when compared to females in placebo treated RmTBI group, $F(1, 27) = 4.393$, $p = .047$, (Fig. 3G).

3.4. Bone density

3.4.1. Males

Antibiotic administration and RmTBI differentially modified bone volume fraction of low-, mid-, and high-density bone within the distal metaphysis of femurs from adolescent males, see Fig. 4. Although there were no significant effects for mean bone density, within the low-density bone parameter, RmTBI significantly reduced bone volume ratio in the placebo treated animals, but not in the antibiotic treated group. The two-way ANOVA exhibited a main effect of injury, $F(1, 34) = 6.922$, $p = .013$, and a significant injury by treatment interaction, $F(1, 34) = 8.628$, $p = .006$. For the mid-density measurement, there was a significant treatment by injury interaction, $F(1, 34) = 7.314$, $p = .011$, with post-hoc analyses revealing that density was reduced in placebo + RmTBI animals ($p = .049$), but increased in males that experience both

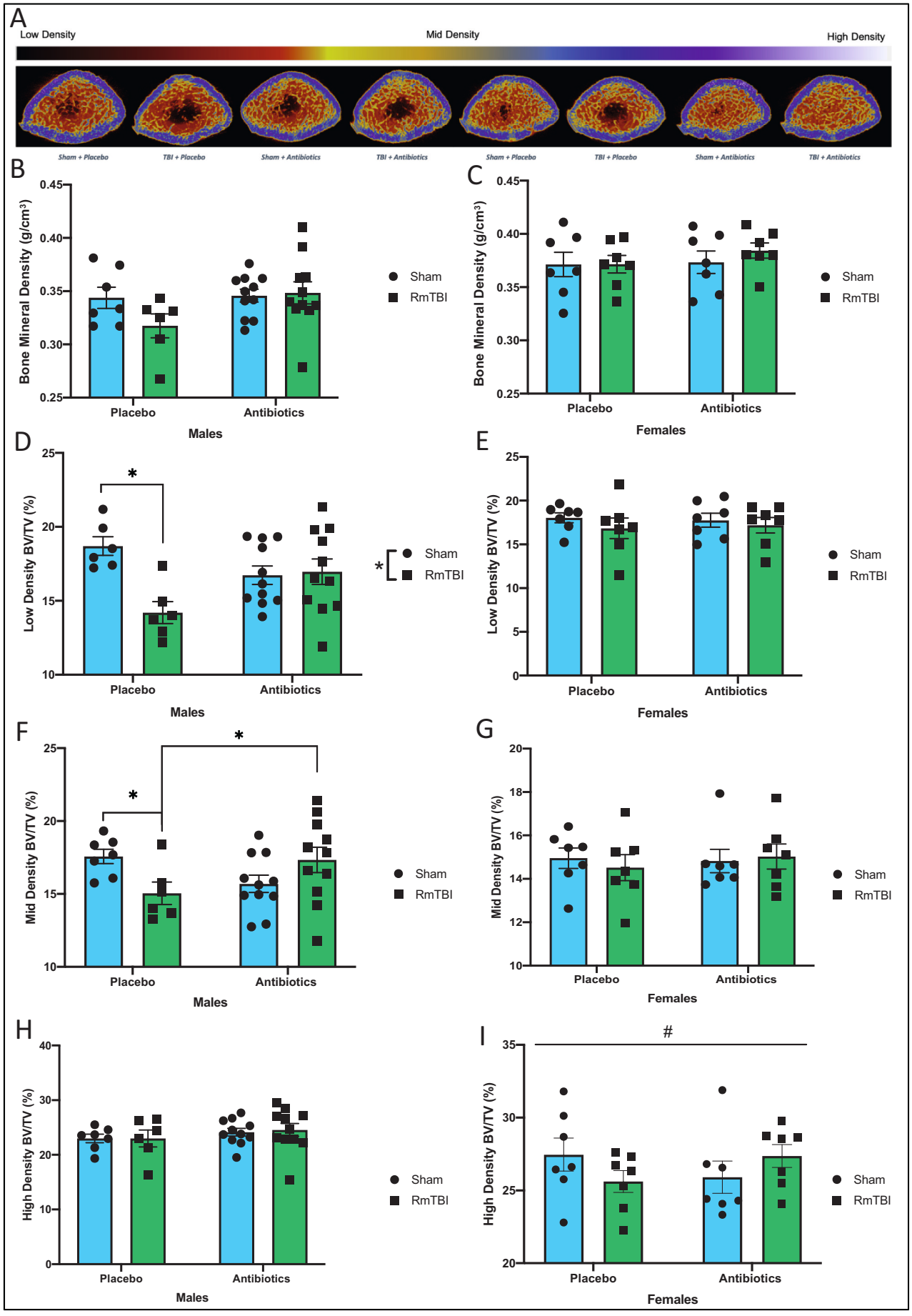

(caption on next page)

Fig. 4. Representative reconstructed cross-sections of femurs from each treatment and injury groups are shown with pseudocolouring density filter (bone and mineral) filter applied to the raw acquired images (A).) Mean bone density failed to exhibit significant main effects for Males (B) and Females (C). Multilevel Otsu threshold levels were calibrated to calcium hydroxyapatite and were used to segregate bone into low density: 0.194–0.548 g/cm^3, mid density: 0.548–0.930 g/cm^3, high density: > 0.930 g/cm^3 for male femurs (D,F,H). There was significantly reduced low density bone for male placebo treated RmTBI rats, when compared to male placebo treated shams. No difference in low density bone was observed within the antibiotic treated group and between treatment groups (D). There was a significant injury effect on mid density bone, where it was reduced in the placebo treated RmTBI rats, when compared to placebo treated shams. There was also treatment effect, where antibiotic treatment increased mid density bone in the antibiotic treated RmTBI rats, compared to placebo treated RmTBI rats (F). There was no difference observed in high density bone (H). Multilevel Otsu threshold levels were calibrated to calcium hydroxyapatite and were used to segregate bone into low density: 0.201–0.576 g/cm^3, mid density: 0.576–0.970 g/cm^3, and high density: > 0.970 g/cm^3 for female femurs (E,G,I). No difference was observed in low (E) and mid density bone (G). There was a significant interaction, where high density bone was reduced in placebo treated RmTBI female rats, when compared to antibiotic treated RmTBI female rats (I). Graphs are shown as mean of each group ± SEM, * represent significant difference, $p < .050$.

antibiotics + RmTBI ($p = .047$). There were no significant modifications in the high-density parameter.

3.4.2. Females

In contrast to adolescent males, in females we observed that only the bone volume fraction of high-density bone was affected (Fig. 4). The two-way ANOVA for bone volume fraction at the high-density parameter demonstrated a significant interaction, $F(1, 28) = 4.792$, $p = .039$, whereby bone volume fraction was reduced in placebo + RmTBI animals, but increased in females that experience both antibiotics + RmTBI. The two-way ANOVAs for low and mid bone density failed to exhibit any significant main effects or interactions, p's > 0.050.

3.5. Mean polar moment of inertia

Male rats exhibited significantly greater mean polar moment of inertia levels than female rats ($p < .001$). However, when two-way ANOVAs were run for male and female rats separately, with injury and treatment as factors, there were no significant effects or interactions in either sex (Fig. 5).

4. Discussion

This study was designed to examine the impact of a 14-day depletion of the gut microbiota prior to RmTBIs on adolescent bone volume and femur length. Our bacterial DNA results indicate that the antibiotic cocktail depleted the adolescent microbiome, while the time-to-right findings show significant loss of consciousness due to injury in the RmTBI group. Consistent with previous studies we found that, even in adolescence, males exhibit stronger bones than females (greater polar moment of inertia). Although male bone development is protracted compared to females, this increased strength likely results from more efficient bone addition to the periosteal surface (Schoenau et al., 2001). Interestingly, in response to our experimental manipulations, bone growth in male and female adolescent rats exhibited sex-dependent changes, with female femur length being reduced in response to both RmTBI and microbiome depletion (but not when combined), while male femur length was only restricted by microbiome depletion. Conversely, in males, CSA, and bone volume fraction of low- and mid-density bone were reduced in those that experienced RmTBIs. However, in females CSA was reduced in microbiome depleted rats but not in microbiome depleted rats given RmTBIs. In addition, only the high-density measurement was modified in females, again being reduced in response to both RmTBI and microbiome depletion (but not when combined).

4.1. Influence of gut microbiome depletion and RmTBI on male femur length

Given that adolescence is a critical period in gut microbiota and skeletal bone growth, it was not surprising that microbiome depletion reduced femur growth in adolescent males that experienced either sham or RmTBIs. There are numerous mechanisms by which the microbiome has been postulated to regulate bone growth including, the SCFA regulation of Insulin Growth Factor-1 (IGF-1) (Medina-Gomez, 2018), production of pro- and anti-inflammatory cytokines (IL-6, IL-1β, TNF-α) (Hernandez et al., 2016) and sex hormones (Imai et al., 2009), regulation of immune cells (T-cells and dendritic cells) (Ke et al., 2019), and importantly nutrient absorption (Chen et al., 2017). For example, gut dysbiosis is not only involved in proinflammatory cytokine production, which reduces calcium absorption (Ding et al., 2020), but also the activation of CD4$^+$ T cells, both of which stimulate of NF-kβ ligands and bone resorption, thereby altering bone growth (Hernandez et al., 2016;

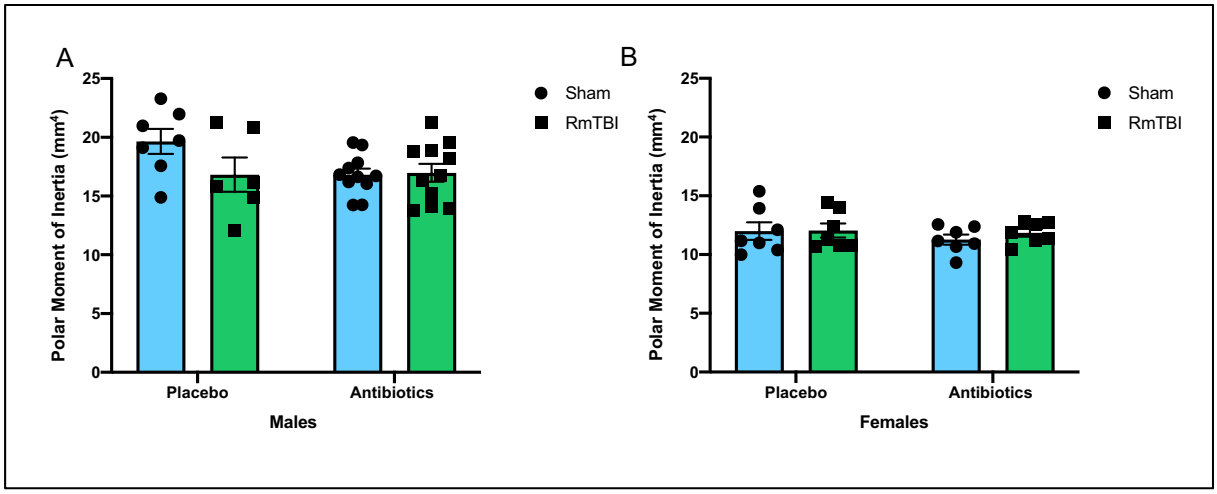

Fig. 5. Illustrative representation of polar moment of inertia measures for male (A) and female (B) rats exposed to placebo or antibiotic treatment, in addition to sham or RmTBIs. Although there was a significant difference between males and females (males > females), treatment and injury did not significantly influence polar moment of inertia. Graphs are shown as mean of each group ± SEM, * represent significant difference, $p < .050$.

Li et al., 2007; Cho et al., 2012). Moreover, intestinal microbes are imperative for the biosynthesis of B vitamins, folate, and Vitamin K, all of which play vital roles in the maintenance of bone mass and growth (Saltzman and Russell, 1998). It is therefore possible that alterations to gut microbiome composition altered the absorption of nutrients and calories (Hernandez et al., 2016), thereby leading to a reduction in femoral length. Interestingly, although present in females, we did not identify RmTBI-induced alterations in male femur length. Rapid bone growth in adolescent males typically peaks between 13 and 17 years of age, which is a later than in females (11 and 14 years of age) (Gokhale et al., 1998). This sex-difference may explain the distinct response to RmTBI we identified in femur length in male and female rats.

4.2. Influence of gut microbiome depletion and RmTBI on male bone volume

In contrast to the effects identified in femur length, bone CSA, and the proportion of bone overall, low and mid density bone was reduced in placebo treated males that experienced RmTBIs. This finding is consistent with previous studies which observed a reduction in bone volume fraction 6 weeks after moderate TBI (Brady et al., 2016b; Brady et al., 2015). Within our ROI, the low and mid density bone are where we expect to identify alterations, as this bone is thought to be porous-like and have high metabolic bone activity that is involved in development and remodeling (Bajwa et al., 2018). Inflammation (both within the brain and systemically) is a hallmark characteristic of RmTBI (Barkhoudarian et al., 2011; Mychasiuk et al., 2015), that has also been shown to modify skeletal bone development (Bajwa et al., 2018). Our results are consistent with previous preclinical and clinical studies that have identified increases in osteoclastic activity and reduced bone mass after RmTBI in trabecular and cortical bone (Brady et al., 2015; Smith et al., 2016; Yu et al., 2014a).

Why exactly gut microbiome depletion prior to RmTBI was protective of overall bone area fraction and mid density bone, but not at low density remains unclear. Gut microbiome depletion in adult male C57BL6/J mice that experienced a TBI was found to be neuroprotective (Simon et al., 2020). Hence, it is likely that ameliorating the brain injury attenuates TBI-induced bone loss. The mechanism is yet to be revealed however, the neuroprotective effects observed in mice may indicate that a reduction of certain gut bacteria may downregulate neuroinflammation and promote recovery. For example, the gut microbiome is involved in the production of serotonin (Martin et al., 2020). It is known that osteoblasts have receptors for serotonin, and the binding of serotonin stimulates osteoblastic activity, resulting in a reduction in bone mass (Chen et al., 2017; Mm et al., 2007). Moreover, germ-free mice have been found to exhibit increased bone volume and lower serum serotonin levels (Chen et al., 2017), suggesting that microbiome-dependent serotonin levels play an important role in skeletal bone formation. Depletion of serotonin producing bacteria may therefore reduce serotonin levels, prevent osteoblastic activity, potentially driving the effect we observed where microbiome depletion in combination with RmTBI was protective for bone loss at mid-density. Importantly, some studies indicate that serotonin has a dual-effect; stimulating or inhibiting bone formation, which varied with sex and age, which may explain why we observed differences in mid-density BV/TV in our male and females (Xu et al., 2017; Warden et al., 2005).

We also observed that antibiotic-treated sham male rats had significantly reduced bone CSA, compared to placebo-treated sham male rats. This finding is consistent with previous studies in adult mice where germ-free male mice demonstrated a reduction in femur length and bone volume (Schwarzer et al., 2016; Yan et al., 2016). These findings support the notion that depletion of gut microbiome has a catabolic effect on bone.

4.3. Influence of gut microbiome depletion and RmTBI on female femur length

Our finding in females that microbiome depletion is catabolic to bone development and reduces femur length is congruent with previous studies demonstrating femur length, cortical thickness, and cortical and trabecular bone composition are all reduced in germ-free mice (Schwarzer et al., 2016; Yan et al., 2016). These studies attribute the deficit in bone development to altered growth hormone-insulin-growth factor-1 (GH/IGF-1) axis signaling, that is regulated by gut microbiota (Schoenau et al., 2001; Wrigley et al., 2017). Taken together, these findings provide evidence that the gut microbiome has an anabolic effect on bone growth (Li et al., 2019).

We also identified a significant decrease in femur length in female placebo treated rats who received RmTBIs. This is consistent with another study that found a reduction in bone formation rate and a reduction in bone mass following RmTBI in 10-week-old female mice (Kesavan et al., 2017). Dysregulated bone development following RmTBI occurs in response to disruptions in the GH/IGF-1 axis (Kesavan et al., 2017; Yuen et al., 2020). IGF-1 which acts downstream of GH, is responsible for the anabolic processes of growth and development throughout life (Wrigley et al., 2017), particularly longitudinal bone growth (Olson et al., 2011). Furthermore, IGF-1 is crucial for bone accrual and maturation, and loss of IGF-1 has been attributed to a reduction in bone length and width (Locatelli and Bianchi, 2014). In the current study, we examined adolescent rats, where active longitudinal bone growth is driven by the proliferation of hypertrophic chondrocytes at the growth plate (Rauch, 2012). Therefore, it is possible that RmTBI disrupted the proliferation of hypertrophic chondrocytes that are responsible for longitudinal bone growth.

Paradoxically, female rats given antibiotic treatment and RmTBI displayed no difference in femur length, suggesting that bone growth was not disrupted following depletion of the gut microbiome when combined with RmTBI. Although numerous studies have demonstrated the negative effect of TBI on bone health in murine (Yu et al., 2014a; Kesavan et al., 2017; Yu et al., 2014b) and rodent (Brady et al., 2016b; Brady et al., 2015) models, the underlying mechanisms remain to be elucidated. Importantly, the studies which observed bone loss following TBI, utilized animals which have unperturbed gut microbiota. In contrast, our study found increased bone formation in female rats that underwent RmTBI but had depleted gut microbiomes. Accumulating evidence suggests the absence of the microbiome may have attenuated neuroinflammation, BBB permeability, peripheral inflammatory response, and sympathetic outflow (Otto et al., 2020), thereby reducing the effect on bone loss. Taken together, the lack of differences in femur length in female rats given antibiotic treatment and RmTBI compared to placebo treated sham rats may support the notion that the microbiome mediates the effects of TBI on bone development. Future studies, however, are required to determine role of each specific bacterial strain on bone formation.

4.4. Influence of gut microbiome depletion and RmTBI on female bone volume

In females we found that antibiotic-treated sham rats had significantly reduced bone CSA and overall bone area fraction when compared to placebo-treated shams. Subsequent analyses revealed that overall bone area fraction as well as high density bone was reduced in female placebo treated rats that experienced RmTBI, when compared to females that had combined injury and treatment. Sex specific changes in mid density bone in males and high-density bone in females may be due to differences in levels of circulating sex hormones affecting bone maturation. These contrasting results indicate that sex-specific effects on bone via microbiota may be driven by sex hormones (Yan and Charles, 2017). Furthermore, it has been established that bone growth and accrual of peak bone mass typically occurs sooner in females than males,

resulting in disparate bone mass beginning at the onset of pubertal maturation (Gokhale et al., 1998; Rizzoli and Bonjour, 1999). This is evidenced by the increased mineral density for females as calculated via the otsu method for the three levels of mineralization when compared to males. Therefore, it is likely that the antibiotic and injury effects are more pronounced at the high-density range in adolescent females who have more high-density bone which is denser than male rats at this timepoint.

5. Conclusion

We identified sexually dimorphic changes in adolescent bone development in response to microbiome depletion and RmTBI. Given the large number of adolescents who experience RmTBIs and microbiome dysbiosis, these findings may have important implications for clinical practices regarding bone development, and therefore require further investigation. It would be imperative for future studies to confirm these findings histologically and elucidate the mechanisms underlying these experience dependent changes, with a specific focus on inflammation (systemic and within the brain), the role of SCFAs and sex hormones, regulation of the GH/IGF-1 axis, and nutrient absorption within the gut. Moreover, as research indicates that the muscular system is a significant modulator of bone development in puberty (Schoenau et al., 2000), future studies could examine the corresponding role of the microbiome and RmTBI on maturation of specific muscles. Finally, given that dietary manipulations, such as supplementation with specific bacterial strains, probiotics, and/or prebiotics, have been shown to modulate the gut microbiota and restore microbiome dysbiosis, diet may be an easy therapeutic avenue to improve bone health following RmTBI.

CRediT authorship contribution statement

All authors contributed to the writing of the manuscript. Ker Rui Wong, Marissa Sgro, Richelle Mychasiuk, Rhys D Brady: Conceptualization, study design, tissue collection, data analysis. Richelle Mychasiuk, Stuart J. McDonald, Sandy R. Shultz: Funding acquisition. Glenn Yamakawa, Crystal Li: Tissue collection.

Declaration of competing interest

Authors declare no competing interest.

Acknowledgements

RM, SJM, and SRS are supported by funding from the Australian National Health and Medical Research Council.

References

Bajwa, N.M, Kesavan, C., Mohan, S., 2018. Long-term Consequences of Traumatic Brain Injury in Bone Metabolism. Front. Neurol, 9:115.
Barkhoudarian, G., Hovda, D.A., Giza, C.C., 2011. The molecular pathophysiology of concussive brain injury. Clin. Sports Med. 30, 33–48. https://doi.org/10.1016/j.csm.2010.09.001.
Bonaz, B., Bazin, T., Pellissier, S., 2018. The Vagus Nerve at the Interface of the Microbiota-Gut-Brain Axis. Front. Neurosci, 12:49.
Borre, Y.E., et al., 2014. Microbiota and neurodevelopmental windows: implications for brain disorders. Trends Mol. Med. 20, 509–518. https://doi.org/10.1016/j.molmed.2014.05.002.
Brady, R.D., et al., 2015. Experimental traumatic brain injury induces bone loss in rats. J. Neurotrauma 33, 2154–2160. https://doi.org/10.1089/neu.2014.3836.
Brady, R., et al., 2016. Experimental traumatic brain injury induces bone loss in rats. J. Neurotrauma 33, 2154–2160.
Brady, R., et al., 2016. Sodium selenate treatment mitigates reduction of bone volume following traumatic brain injury in rats. J. Musculoskelet. Neuronal Interact. 16, 369.
Chen, K.L., Madak-Erdogan, Z., 2016. Estrogen and microbiota crosstalk: should we pay attention? Trends in Endocrinology & Metabolism 27, 752–755.
Chen, Y.C., Greenbaum, J., Shen, H., Deng, H.W., 2017. Association between gut microbiota and bone health: potential mechanisms and prospective. J. Clin. Endocrinol. Metab. 102, 3635–3646. https://doi.org/10.1210/jc.2017-00513.
Cho, I., et al., 2012. Antibiotics in early life alter the murine colonic microbiome and adiposity. Nature 488, 621–626. https://doi.org/10.1038/nature11400.
Cohen, J., 1992. Statistical power analysis. Curr. Dir. Psychol. Sci. 1, 98–101.
Cowan, C.S.M., Dinan, T.G., Cryan, J.F., 2020. Annual research review: critical windows – the microbiota–gut–brain axis in neurocognitive development. J. Child Psychol. Psychiatry. https://doi.org/10.1111/jcpp.13156.
Ding, K., Hua, F., Ding, W., 2020. Gut microbiome and osteoporosis. Aging Dis. 11, 438–447. https://doi.org/10.14336/AD.2019.0523.
Erny, D., et al., 2015. Host microbiota constantly control maturation and function of microglia in the CNS. Nat. Neurosci. 18, 965–977. https://doi.org/10.1038/nn.4030.
Gokhale, R., et al., 1998. Bone mineral density assessment in children with inflammatory bowel disease. Gastroenterology 114, 902–911. https://doi.org/10.1016/s0016-5085(98)70309-9.
Hernandez, C.J., Guss, J.D., Luna, M., Goldring, S.R., 2016. Links between the microbiome and bone. J. Bone Miner. Res. 31, 1638–1646. https://doi.org/10.1002/jbmr.2887.
Hoban, A.E., et al., 2016. Behavioural and neurochemical consequences of chronic gut microbiota depletion during adulthood in the rat. Neuroscience 339, 463–477. https://doi.org/10.1016/j.neuroscience.2016.10.003.
Ibáñez, L., Rouleau, M., Wakkach, A., Blin-Wakkach, C., 2019. Gut microbiome and bone. Joint Bone Spine 86, 43–47. https://doi.org/10.1016/j.jbspin.2018.02.008.
Imai, Y., et al., 2009. Estrogens maintain bone mass by regulating expression of genes controlling function and life span in mature osteoclasts. Ann. N. Y. Acad. Sci. 1173 (Suppl. 1), E31–E39. https://doi.org/10.1111/j.1749-6632.2009.04954.x.
Jin, W., et al., 2008. Increased intestinal inflammatory response and gut barrier dysfunction in Nrf2-deficient mice after traumatic brain injury. Cytokine 44, 135–140. https://doi.org/10.1016/j.cyto.2008.07.005.
Ke, K., Arra, M., Abu-Amer, Y., 2019. Mechanisms underlying bone loss associated with gut inflammation. Int. J. Mol. Sci. 20, 6323. https://doi.org/10.3390/ijms20246323.
Kesavan, C., Bajwa, N.M., Watt, H., Mohan, S., 2017. Experimental repetitive mild traumatic brain injury induces deficits in trabecular bone microarchitecture and strength in mice. Bone Res. 5, 1–10.
Li, Y., et al., 2007. B cells and T cells are critical for the preservation of bone homeostasis and attainment of peak bone mass in vivo. Blood 109, 3839–3848. https://doi.org/10.1182/blood-2006-07-037994.
Li, J.Y., et al., 2016. Sex steroid deficiency-associated bone loss is microbiota dependent and prevented by probiotics. J. Clin. Invest. 126, 2049–2063. https://doi.org/10.1172/jci86062.
Li, L., et al., 2019. Microbial osteoporosis: the interplay between the gut microbiota and bones via host metabolism and immunity. MicrobiologyOpen 8, e00810.
Locatelli, V., Bianchi, V.E., 2014. Effect of GH/IGF-1 on bone metabolism and osteoporsosis. Int. J. Endocrinol. 2014.
Martin, A.M., Jones, L.A., Jessup, C.F., Sun, E.W., Keating, D.J., 2020. Diet differentially regulates enterochromaffin cell serotonin content, density and nutrient sensitivity in the mouse small and large intestine. Neurogastroenterol. Motil. 32, e13869.
Medina-Gomez, C., 2018. Bone and the gut microbiome: a new dimension. J. Lab. Precis. Med. 3.
Mm, B., et al., 2007. Serotonin transporter and receptor expression in osteocytic MLO-Y4 cells. Bone 39, 1313–1321. https://doi.org/10.1016/j.bone.2006.06.009.
Mychasiuk, R., Hehar, H., van Waes, L., Esser, M.J., 2015. Diet, age, and prior injury status differentially alter behavioral outcomes following concussion in rats. Neurobiol. Dis. 73, 1–11. https://doi.org/10.1016/j.nbd.2014.09.003.
Mychasiuk, R., Hehar, H., Candy, S., Ma, I., Esser, M.J., 2016. The direction of the acceleration and rotational forces associated with mild traumatic brain injury in rodents effect behavioural and molecular outcomes. J. Neurosci. Methods 257, 168–178. https://doi.org/10.1016/j.jneumeth.2015.10.002.
Olson, L.E., Ohlsson, C., Mohan, S., 2011. The role of GH/IGF-I-mediated mechanisms in sex differences in cortical bone size in mice. Calcif. Tissue Int. 88, 1–8.
Otsu, N., 1979. A threshold selection method from gray-level histograms. IEEE Trans. Syst. Man Cybern. 9, 62–66.
Otto, E., et al., 2020. Crosstalk of brain and bone—clinical observations and their molecular bases. Int. J. Mol. Sci. 21, 4946.
Paus, T., Keshavan, M., Giedd, J.N., 2008. Why do many psychiatric disorders emerge during adolescence? Nat. Rev. Neurosci. 9, 947–957. https://doi.org/10.1038/nrn2513.
Rauch, F., 2012. The dynamics of bone structure development during pubertal growth. J. Musculoskelet. Neuronal Interact. 12, 1–6.
Rauch, F., Schoenau, E., 2001. Changes in bone density during childhood and adolescence: an approach based on bone's biological organization. J. Bone Miner. Res. 16, 597–604. https://doi.org/10.1359/jbmr.2001.16.4.597.
Rizzoli, R., Bonjour, J., 1999. Determinants of peak bone mass and mechanisms of bone loss. Osteoporos. Int. 9, S17.
Rosenbaum, S.B., Lipton, M.L., 2012. Embracing chaos: the scope and importance of clinical and pathological heterogeneity in mTBI. Brain Imaging Behav. 6, 255–282.
Saltzman, J.R., Russell, R.M., 1998. The aging gut: nutritional issues. Gastroenterol. Clin. N. Am. 27, 309–324.
Schoenau, E., Neu, C., Mokov, E., Wassmer, G., Manz, F., 2000. Influence of puberty on muscle area and cortical bone area of the forearm in boys and girls. J. Clin. Endocrinol. Metab. 85, 1095–1098.
Schoenau, E., Neu, C., Rauch, F., Manz, F., 2001. The development of bone strength at the proximal radius during childhood and adolescence. J. Clin. Endocrinol. Metab. 86, 613–618.
Schwarzer, M., et al., 2016. Lactobacillus plantarum strain maintains growth of infant mice during chronic undernutrition. Science 351, 854–857.

Simon, D.W., et al., 2020. Depletion of gut microbiota is associated with improved neurologic outcome following traumatic brain injury. Brain Res. 1747, 147056 https://doi.org/10.1016/j.brainres.2020.147056.
Smith, É., Comiskey, C., Carroll, Á., 2016. Prevalence of and risk factors for osteoporosis in adults with acquired brain injury. Irish J. Med. Sci. 185, 473–481. https://doi.org/10.1007/s11845-016-1399-5.
Strandwitz, P., 2018. Neurotransmitter modulation by the gut microbiota. Brain Res. 1693, 128–133. https://doi.org/10.1016/j.brainres.2018.03.015.
Sudo, N., et al., 2004. Postnatal microbial colonization programs the hypothalamic-pituitary-adrenal system for stress response in mice. J. Physiol. 558, 263–275. https://doi.org/10.1113/jphysiol.2004.063388.
Walker, E.C., et al., 2020. Cortical bone maturation in mice requires SOCS3 suppression of gp130/STAT3 signalling in osteocytes. elife 9, e56666.
Walker, E., McGregor, N., Chan, A., Sims, N., 2021. Measuring bone volume at multiple densities by micro-computed tomography. Bio-Protocol 11, e3873.
Warden, S.J., Robling, A.G., Sanders, M.S., Bliziotes, M.M., Turner, C.H., 2005. Inhibition of the serotonin (5-hydroxytryptamine) transporter reduces bone accrual during growth. Endocrinology 146, 685–693. https://doi.org/10.1210/en.2004-1259.
Williams, J.A., Windmill, J.F., Tanner, K.E., Riddell, J.S., Coupaud, S., 2020. Global and site-specific analysis of bone in a rat model of spinal cord injury-induced osteoporosis. Bone Rep. 12, 100233.
Wrigley, S., Arafa, D., Tropea, D., 2017. Insulin-like growth factor 1: at the crossroads of brain development and aging. Front. Cell. Neurosci. 11, 14.
Xu, X., et al., 2017. Intestinal microbiota: a potential target for the treatment of postmenopausal osteoporosis. Bone Res. 5, 17046. https://doi.org/10.1038/boneres.2017.46.
Yan, J., Charles, J.F., 2017. Gut microbiome and bone: to build, destroy, or both? Curr. Osteoporos. Rep. 15, 376–384. https://doi.org/10.1007/s11914-017-0382-z.
Yan, J., et al., 2016. Gut microbiota induce IGF-1 and promote bone formation and growth. Proc. Natl. Acad. Sci. U. S. A. 113, E7554–e7563. https://doi.org/10.1073/pnas.1607235113.
Yu, H., Watt, H., Mohan, S., 2014. The negative impact of traumatic brain injury (TBI) on bone in a mouse model. Brain Inj. 28, 244–251. https://doi.org/10.3109/02699052.2013.859735.
Yu, H., Wergedal, J.E., Rundle, C.H., Mohan, S., 2014. Reduced bone mass accrual in mouse model of repetitive mild traumatic brain injury. J. Rehabil. Res. Dev. 51, 1427–1437.
Yuen, K.C., et al., 2020. Alterations of the GH/IGF-I axis and gut microbiome after traumatic brain injury: a new clinical syndrome? J. Clin. Endocrinol. Metab. 105, e3054–e3064.
Yurkovetskiy, L., et al., 2013. Gender bias in autoimmunity is influenced by microbiota. Immunity 39, 400–412.